CONCRETE PARTICLE CHARACTERIZATION

USING IMPEDANCE CYTOMETRY

by

KAVYA VASUDEVAMURTHY

A Thesis submitted to the

School of Graduate Studies

Rutgers, the State University of New Jersey

in partial fulfillment of the requirements

for the degree of

Master of Science

Graduate Program in Electrical and Computer Engineering

Written under the direction of

Mehdi Javanmard

and approved by

_____

_____

_____

_____

New Brunswick, New Jersey

October 2018

ABSTRACT OF THE THESIS

CONCRETE PARTICLE CHARACTERIZATION USING IMPEDANCE CYTOMETRY

by KAVYA VASUDEVAMURTHY

THESIS DIRECTOR:
Dr. Mehdi Javanmard

We demonstrate a novel method to detect and characterize the size and number of Wollastonite particles using microfluidic impedance cytometry. The fabricated device which consists of gold electrodes micro-fabricated in a microchannel is capable of detecting particles >1 micron. Particle characterization is often carried out across a wide range of industries and is a critical parameter in the manufacture of various products to help improve the characteristics, performance or quality of powders or particles. There are a number of commercially available particle characterization techniques like laser diffraction, dynamic light scattering, electrophoretic light scattering, automated imaging,

sedimentation etc that can be used to measure particulate samples and each has its relative strengths and limitations-there is no universally applicable technique for all samples. Our approach uses electrical impedance spectroscopy which measures the change in impedance as the particles in suspension pass through the sensor. It is a highly precise, low cost alternative for particle size characterization with a smaller footprint offering quick analysis time and is suitable for relatively broad range of particle sizes.

ACKNOWLEGMENTS

I would like to begin by thanking Dr. Mehdi Javanmard for being a great mentor and giving me the opportunity to work in his amazing facility here at the Nano Bioelectronics Laboratory. His guidance proved invaluable through the course of my thesis project and my Masters' Degree.

I am grateful to PhRMA foundation for funding this work. I would like to specially thank my co-advisor from Rutgers University-Department of Material Science and Engineering, Dr. Richard Riman for his support and valuable insights as well as providing samples for this project. I am also grateful to all members of Microelectronics Research Laboratory (MERL) at Rutgers University for assisting me in the fabrication processes.

I am thankful to Dr. Laleh Najafizadeh and Dr. Zoran Gajic for being a part of my Masters' Thesis committee, whose feedback will be immensely helpful.

Special thanks to all the members of my lab: Jianye Sui, Karan Ahuja, Tuan Le, Pengfei Xie, Sakshi Sardar, Zhongtian Lin and Azam Gholizadeh for their contributions and timely help.

I extend my thanks to John Scafidi, Arletta Hoscilowicz, Pamela Heinold, Christy Lafferty, Steve Orbine and Robert Lorber.

I would like to mention my parents for their unwavering support and keeping me motivated in trying times. Finally, I am thankful to my friends and all the faculty who served as a constant motivation for me to excel.

TABLE OF CONTENTS

LIST OF FIGURES

Chapter 1

Introduction

1.1 Coulter Counters

For several decades Coulter Counters have been a vital instrument in biological cell detection and enumeration. They are widely used in medical diagnostics for characterization of cells and colloidal particles [1]. Recent advances have led to the application in analysis in various biological particles [2] including human cells [3], DNA [4,5], bacteria [6], viruses [7,8], pollen [9,10] and other bio-molecules [11]. Coulter counters offer simplicity and ruggedness of design with low power consumption and the ability to detect a single particle. Figure 1.1 shows an image of the Multisizer 4e Coulter Counter by Beckman Coulter® providing complex sample analysis across a wide particle sizes ranging from 0.2µm.

Fig 1.1 Multisizer 4e Coulter Counter by Beckman Coulter Life Sciences®

A typical coulter counter [12] also known as a resistive pulse sensor consists of an electrolyte-filled chamber with an aperture and a pair of sensing electrodes on each side of the channel. The size of the aperture is varied to cover various size ranges. Restrictions on buffer conductivity varies with size of the aperture tube as it affects the dynamic range. Applying a voltage across the electrodes when a particle passes through the aperture causes a change in the electrical resistance as it displaces the conductive fluid in the channel. By characterizing this impedance-based detection method corresponding to the size, shape and mobility of the particle passing by can be determined [22][26]. For microfabricated devices the electrodes are usually made of gold or platinum and are smaller in size because of which the effects of electrode polarization at the electrode-electrolyte interface due to the formation of an electrical double layer cannot be ignored [13]. This double layer is electrically modeled as capacitances in series with the electrolyte resistance in the microchannel. Particle sizes are often wrongly estimated in comparison to their actual sizes for dc coulter counters since a large portion of applied voltage is lost across the double layers and only a small portion appears across the channel resistance if the polarization effect is not considered [13][15][32]. However, for ac measurements, the effect of electrode polarization is reduced as the impedance of double layer decreases with frequency.

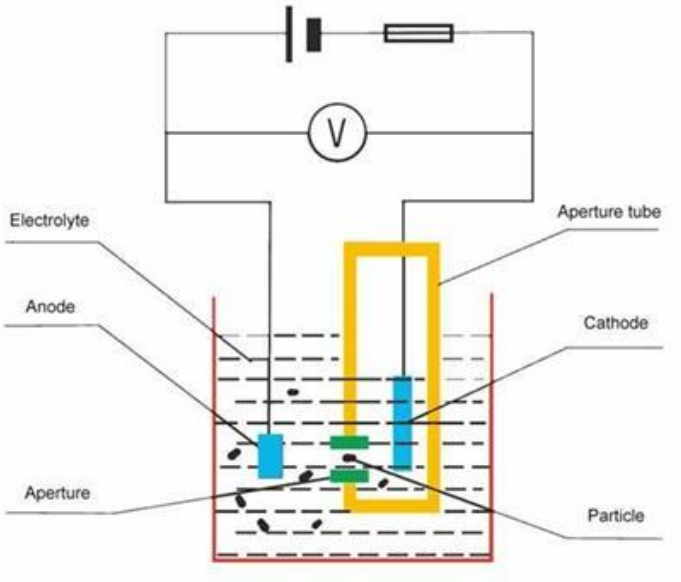

Fig 1.2 Schematic of a coulter counter

The Coulter principle is not a perfect tool and it is important to choose the right model for the desired applications such as counting or sizing of particles to ensure high accuracy and precision. Some models are solely designed for cell counting purposes and lack the advanced circuitry required for sizing particles. Each model is optimized for specific functions such as characterization of human blood cells, counting of a wide variety of cells including bacteria, plant cell aggregates and fat cells. This principle has also been applied to a variety of fields beyond cellular studies for nanoparticle characterization. In this work, we apply this coulter counter principle for the rapid characterization of concrete powders.

1.2 Particle Properties

At the most basic level, a particle can be defined as a discrete sub-portion of a substance. The most common types of materials consisting of particles are powders and granules, suspensions, emulsions, aerosols and sprays. It is vital to measure particle properties in order to maintain better control over the product quality and to have better understanding of products, ingredients and processes. Often, in addition to chemical composition, the physical properties of the constituent particles dominate the behavior of particulate materials. These properties can influence several material properties including rate of dissolution and reaction, ease of flow and mix of ingredients, abrasivity and compressibility. From the perspective of development and manufacturing, some of the most important physical properties required to be measured are particle size and shape, it's surface and mechanical properties, microstructure and charge properties. Based on the material of interest, some or all of these properties may be of importance and interrelated for example, particle size and surface area. For the purpose of this research, we will focus on measuring one of the critical and most significant physical property which is the size of the particle. Particles are said to be 3-dimensional objects and they cannot be described by a single dimension such as radius unless they are perfectly spherical. The size of a particle influences material properties such as texture and feel, appearance, viscosity, suspension stability etc. Particle size measurement and understanding how it affects each product and its manufacturing process is a critical parameter to the success of manufacturing.

1.3 Research Goals

Particle size distribution provides information for the majority of particle characterization applications although some techniques are higher resolution than the others. Ensemble technologies such as laser diffraction and dynamic light scattering are powerful techniques that are “resolution limited” compared to high resolution techniques which are based on particle counting such as electro zone counting or image analysis. Various criteria such as desired particle property, particle size range, sample quantity and analysis time, sample dispersion and its method of preparation, distribution resolution, sensitivity and cost must be considered when deciding the particle characterization technique to be used. Despite significant achievement, each of the current particle sizing equipment have their own drawbacks with bulky instrumentation and a cost range of $30,000 to $100,000.

Therefore, there arises the need to develop a low cost, compact and portable device for particle size characterization. In this work, our goal was to fabricate and characterize a device capable of detecting particles in wet dispersion using multi-frequency impedance cytometry.

Microfluidic impedance-based cytometry has advantages of being label-free, compatibility for mass manufacturing, inexpensive, requirement of low sample volume and it can be miniaturized into a small instrument with tiny foot print.

1.4 Thesis Organization

Chapter 2 presents an overview of current techniques for particle size analysis. We briefly discuss the laser diffraction method, dynamic light scattering and electrical zone sensing. We also look at the commercially available product for particle characterization and the advantages of each technique.

Chapter 3 focuses on our novel approach to analyze particle size. Firstly, we discuss in brief about impedance cytometry in chapter 3.1. In chapter 3.2, we look at the steps involved in fabrication and integration of our sensor device. Chapter 3.3 focuses the sample used for our approach and its preparation. Chapter 3.4 electrical impedance cytometry and chapter 3.5 on signal processing.

In Chapter 4, the results of our technique are presented along with further discussions on our approach.

Finally, in Chapter 5, the conclusions and future scope are discussed. We discuss how this novel approach can be improvised. We also present how impedance cytometry is made portable which can help optimize this method towards particle characterization.

Chapter 2

Particle Size Analysis

2.1 Laser Diffraction Method

For material sizes ranging from hundreds of nanometers to several millimeters, laser diffraction particle sizing technique is widely used. This technique measures the angular variation of scattered light intensity as a laser beam passes through a particle sample dispersion. While small particles scatter light at large angles relative to the laser beam, large particles diffract light at small angles. The size of the particles creating the scattering pattern is measured by analyzing angular scattering intensity data. This method offers wide dynamic range, rapid measurements, high sample throughput and repeatability. Figure 2.1 shows an image of the LA-960 Laser Particle Size Analyzer by HORIBA® with state of the art refinements to measure wet and dry samples measuring 10 nm to 5 mm.

Figure 2.1 LA-960 Laser Particle Size Analyzer by HORIBA®

2.2 Dynamic Light Scattering

Dynamic Light scattering is a well-established and non-invasive technique to measure particle size. It can be used to measure particulate samples in a liquid suspension such as nanoparticles, proteins, polymers and emulsions. It works on the principle that suspended particles undergo Brownian motion as a result of thermally induced collisions between solvent molecules and the particles suspended. If a laser beam is used to illuminate these particles, intensity of scattered light fluctuates and smaller particles move more rapidly as they are displaced further by the solvent molecules. A conventional instrument consists of a laser source which converges using a lens to focus in the sample. Scattered light is collected by a single detector places at 90° to laser beam and the fluctuations in intensity of scattered light are converted to electrical pulses. This is fed to a digital correlator which generates an autocorrelation function that corresponds to particle size. Figure 2.2 illustrates this concept. This technique is ideal for nano and biomaterial, requires small sample quantity, has fast analysis and high throughput allowing for complete sample recovery.

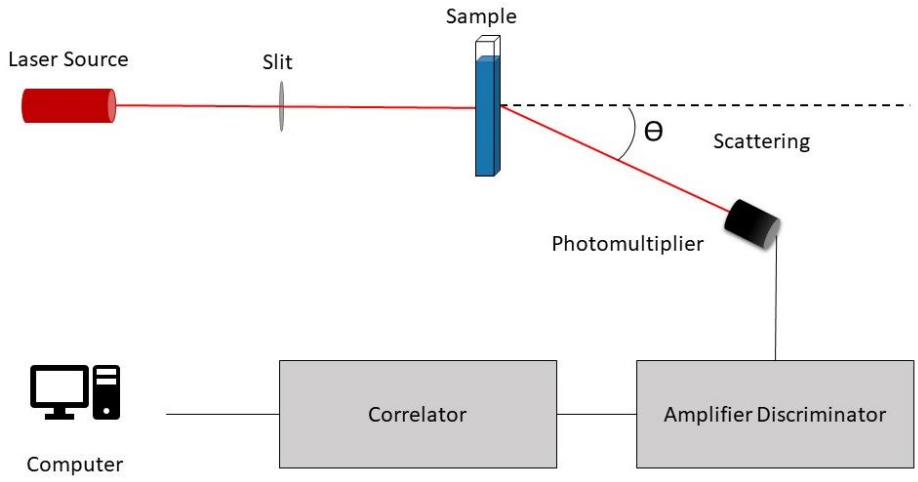

Figure 2.2 Schematic of dynamic light scattering

2.3 Electrical Sensing Zone Method

The Electrical Sensing Zone Method for particle characterization is used for counting and sizing organic and inorganic materials effectively. In comparison to other established methods, the advantageous characteristic of this measurement technique is that is unaffected by samples that have assorted densities, optical properties, shapes and color. It offers a robust, high speed, high resolution and precise instrument suitable for industry as well as research and development laboratories. Figure 2.3 shows a picture of the Elzone® II 5390 Particle Size Analyzer from Micrometrics which utilizes the electrical sensing zone method to size samples.

Figure 2.3 Elzone® II 5390 Particle Size Analyzer from Micrometrics

The Electrical sensing zone method is also referred to as the Counter technique of particle measurement where particles are suspended in a conductive fluid and are drawn through a precision orifice which has platinum electrodes on either side. A constant current is applied to the electrodes which results in a constant voltage across the orifice. As a particle passes through the orifice, it results in a change in electrolyte resistance generating a voltage pulse, the amplitude of which is proportional to the volume of the particle. The size distribution is determined by analyzing one particle at a time providing accurate particle count data as well. Figure 2.4 shows the electrical sensing zone method used in Elzone® II 5390 Particle Size Analyzer from Micrometrics.

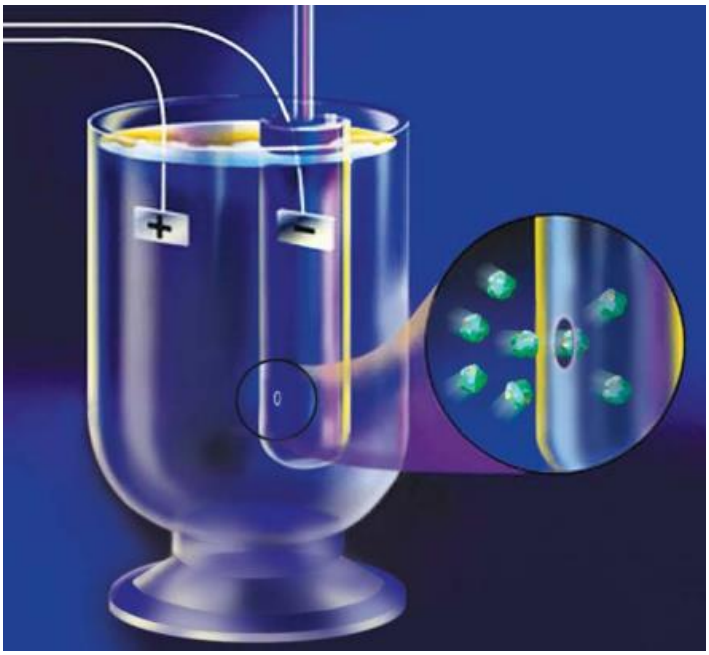

Figure 2.4 Electrical sensing zone method used in Elzone® II 5390 Particle Size Analyzer [41]

Chapter 3

Methodology

3.1 Proposed Approach

Figure 3.1 presents the block diagram of our system. It consists of microfluidic channel bonded onto a glass wafer fabricated with gold electrodes, a multi-frequency lock-in amplifier (Zurich Instruments®) and the software to record and analyze the data. This approach requires only 1 g of dry sample and is ultra-compact eliminating the use of bulky and expensive instrumentation. Each individual block is explained in detail in the following sections.

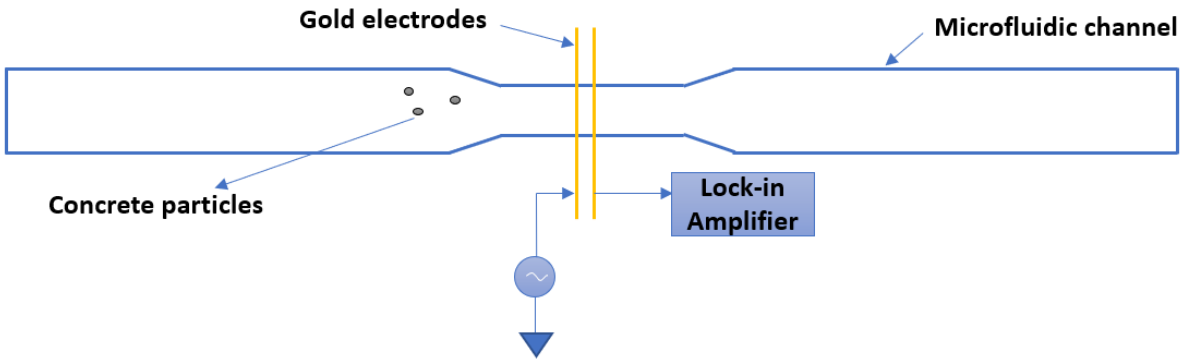

Figure 3.1. Schematic Diagram of the system. Multi-frequency impedance cytometry measures the response across a broad range of frequencies.

3.2 Device Fabrication

Device fabrication for our approach is a four step process, consisting of: fabrication of the sensor, fabrication of master mold for microfluidic channels, soft-lithography and bonding.

3.2.1 Sensor Fabrication

Standard photolithography on a 3” fused silica wafer (University Wafer, Inc) is used to fabricate the electrodes. The first step in this process is to photo-pattern the resist on the silica wafer which involves cleaning the wafer, spin coating the photo-resist AZ5214 (Microchemicals) onto the wafer, soft bake of this resist, exposure to UV light through a 4”x4” chromium mask, developing the resist using AZ5214 MIF Developer, rinse in isopropyl alcohol and blow-dry using nitrogen and finally hard bake of the resist. This photo-patterning step is then followed by deposition of 100nm gold layer onto the wafer using electron beam evaporation. A 10 nm chromium layer is used to enhance the adhesion of the gold layer onto the substrate to prevent wash off during the next step which is liftoff processing. We use gold as the metal to fabricate the electrodes due to its inert nature and resistance to corrosion. Figure 3.2 represents the process involved in sensor fabrication and Figure 3.3 represents the fabricated sensor using this process.

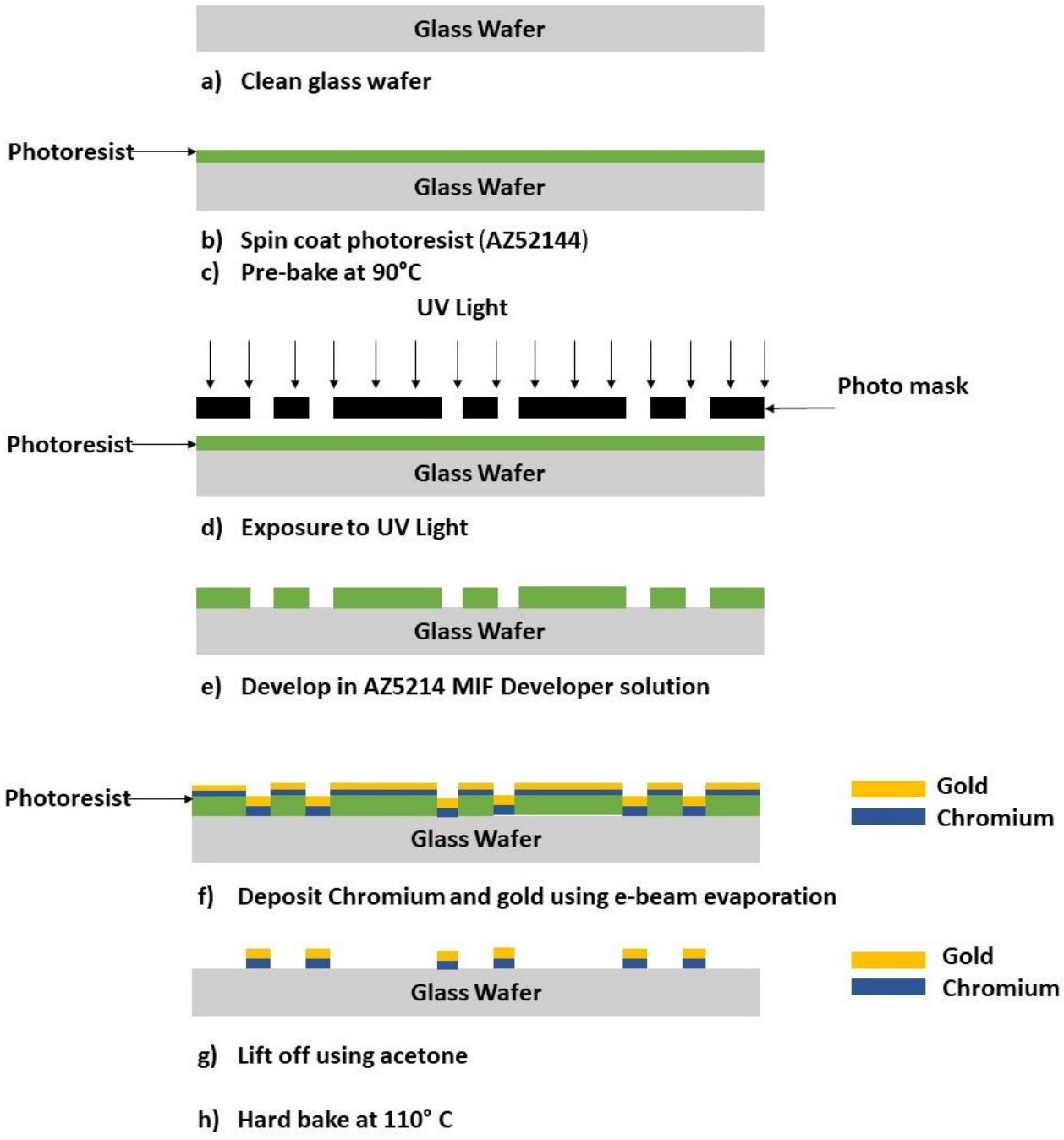

Figure 3.2. Processes involved in sensor fabrication.

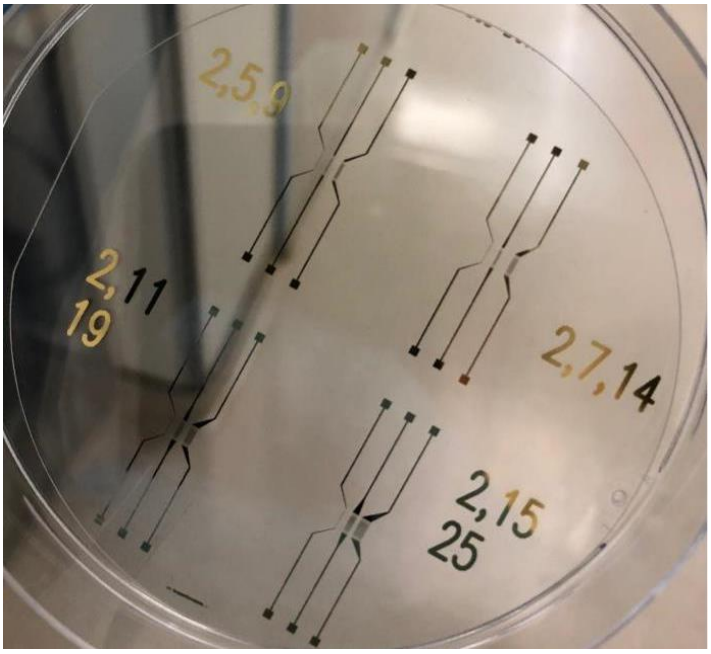

Figure 3.3. Picture of fabricated electrodes. Device also contains multi-electrodes but for our approach we have used the two electrode system.

3.2.2 Fabrication of Master Mold for Microfluidic Channels

The master mold for microfluidic channels is fabricated by photo-patterning a layer of SU-8 on a 3” silicon wafer (University Wafer). This process involves cleaning of the wafer, treating the wafer to oxygen plasma, spin coating the photoresist (Microchemicals), soft bake of this resist, exposure to ultraviolet light through a 4”x4” chromium mask, developing the resist using SU8-10 Developer and hard bake of the resist. SU8-10 is a negative photoresist which means the unexposed region dissolves after development. Exposing the wafer to oxygen plasma after wafer cleaning ensures the even spreading of photoresist as SU8-10 is highly viscous.

Figure 3.4 represents the process involved in the fabrication of master mold and Figure 3.5 presents the fabricated mold using this process. The fabricated microchannel was 28 µm high and 100 µm in width.

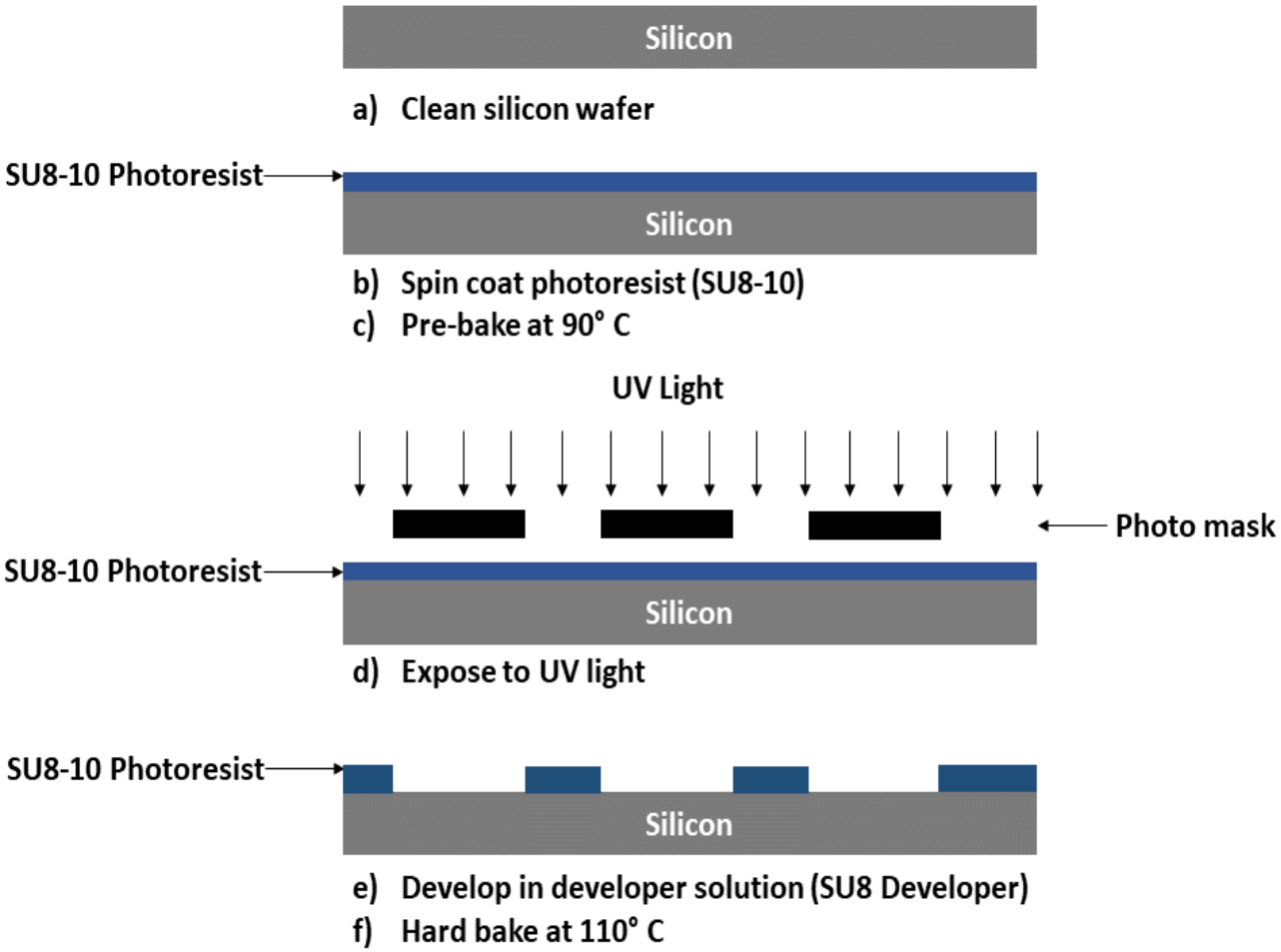

Figure 3.4 Processes involved in fabrication of master mold

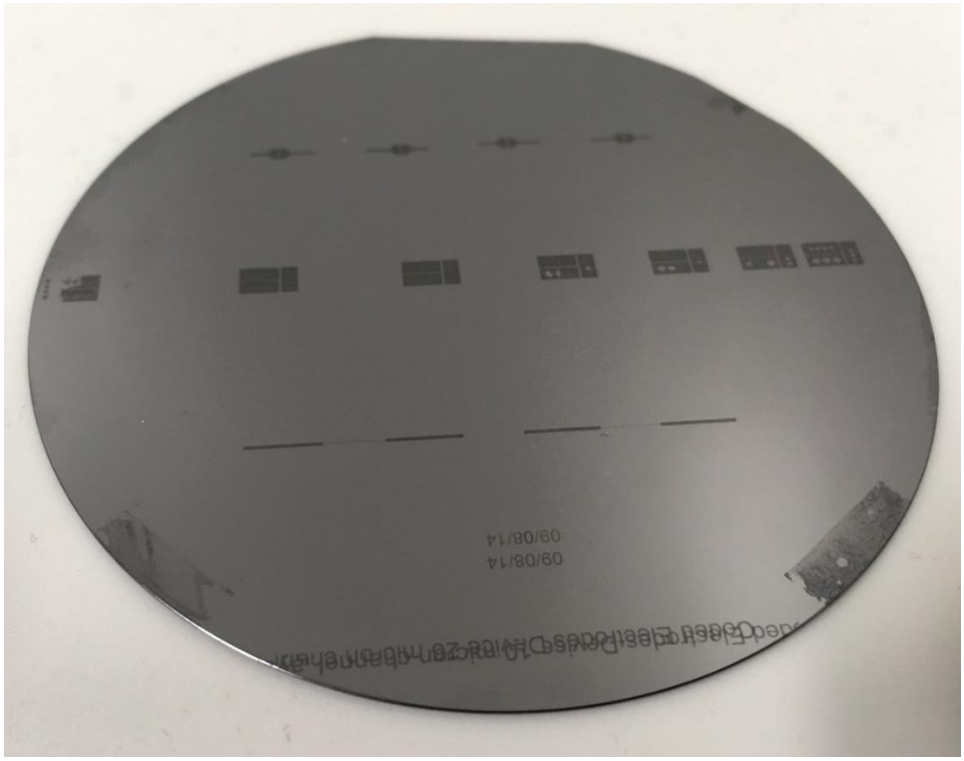

Figure 3.5. Picture of fabricated master mold. Bottom two microfluidic channels are used for our application.

3.2.3 Soft-lithography

Soft-lithography is a method for replica molding suited for micro and nanofabrication. It provides a convenient, low-cost method for applications in biotechnology. Polydimethylsiloxane (PDMS) is the most widely used silicon-based polymer which is moldable elastomer and is optically clear and inert and thus commonly used to make microfluidic channels. Post fabrication of the master mold, PDMS in the ratio 10:1 pre-polymer/ curing agent (Sylgard184 Kit from Dow Corning Corp., MI) was poured onto the

master mold, degassed in a vacuum chamber to remove any air bubbles and cured by baking at 80°C for about 2 hours in order to transfer the patterns to the PDMS layer. After curing, the PDMS channel is peeled off from the mold. Figure 3.6 represents the process involved in soft-lithography.

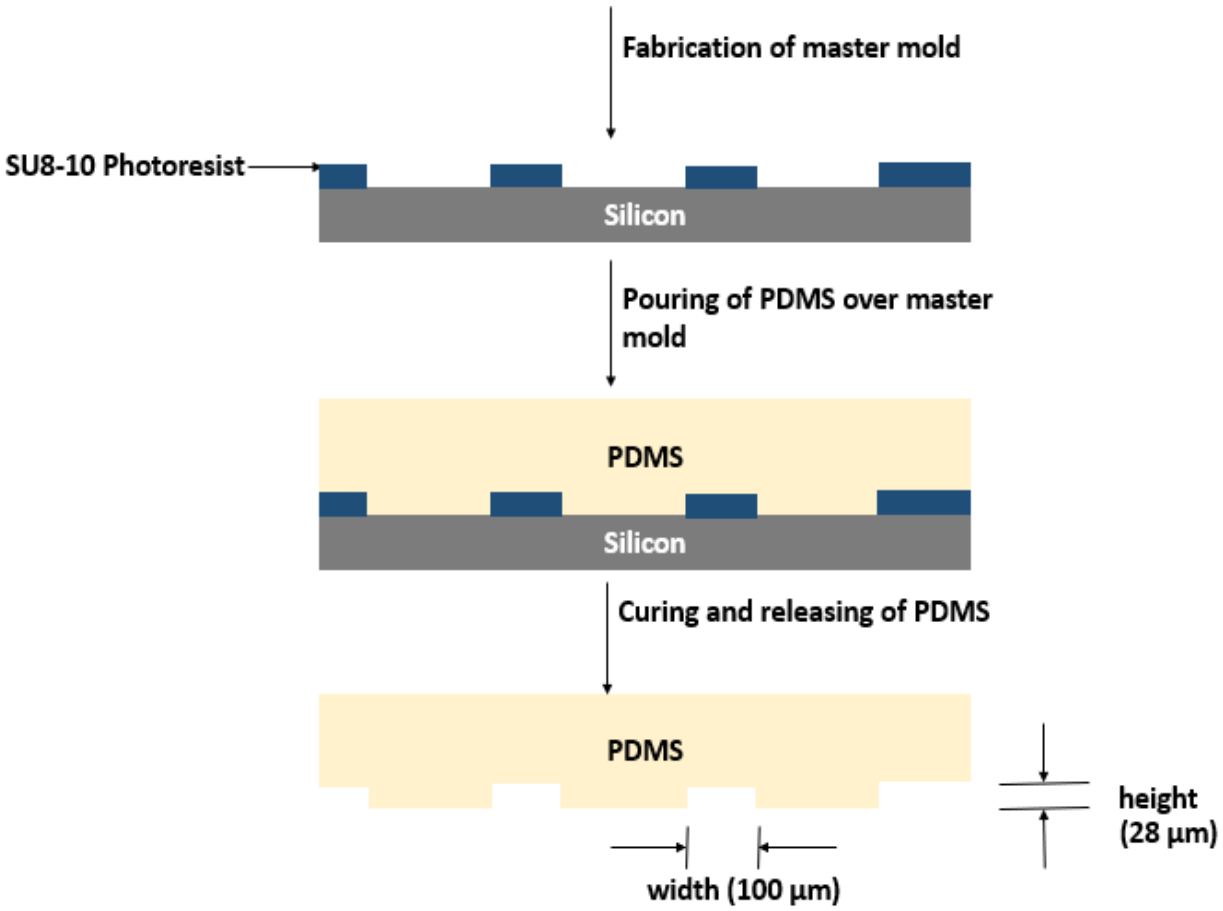

Figure 3.6. Using soft-lithography to create microfluidic channels

3.2.4 Device Bonding

Two wire bonding pads are attached to the electrodes using a mixture of conductive epoxy and hardener (1:1) and kept 24 hours in room temperature for firm bonding. Onto the cured PDMS replica, punch 5mm and 2mm holes for the inlet and outlet of the channel respectively. It is necessary to clean the PDMS substrate with iso-propyl alcohol and the sensors using acetone prior to bonding. We then align the PDMS substrate and the electrode patterned wafer and bond it after both substrates have undergone oxygen plasma treatment. Bake this chip at 65°C (Lab Line® Imperial III Radiant Heat Oven) for 30min to form an irreversible bond. Figure 3.7 represents the bonded device and Figure 3.8 presents microscopic view of microfabricated electrodes bonded with the channel.

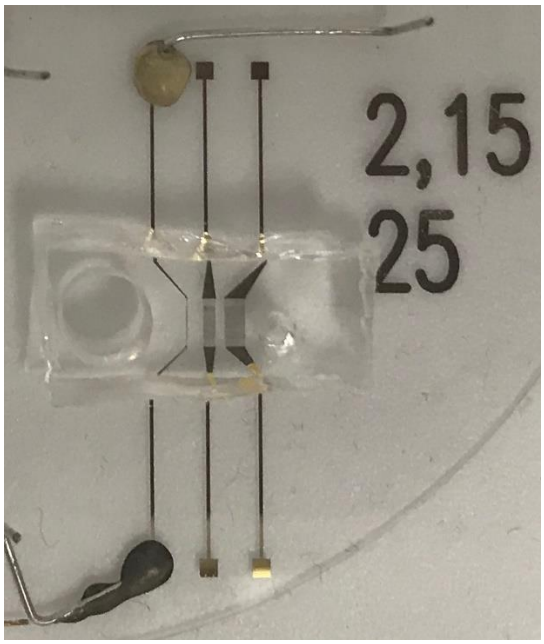

Figure 3.7. Image of PDMS microfluidic channel bonded to electrodes. The two ends of the electrodes are further connected to a multi-frequency lock-in amplifier.

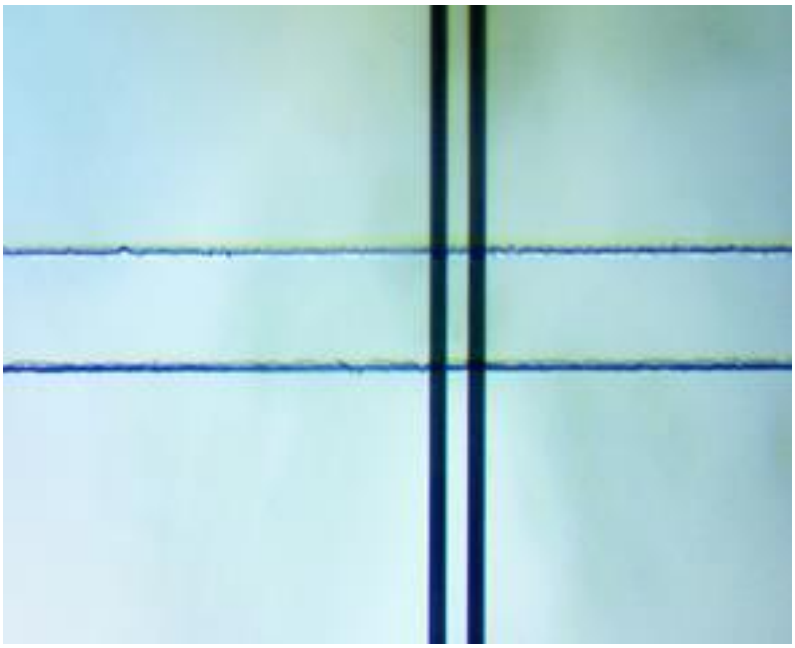

Figure 3.8. Microfabricated electrodes at the channel.

3.3 Concrete particles

We used Wollastonite NYAD® 400 (NYCO® minerals) which is a chemically treated powdered grade material with a median particle size of 8 µm (MICROTRAC) and a surface area of 1.8 m^2/g (BET theory) [42]. Wollastonite is a naturally occurring white mineral with a needle-shaped particle structure and many unique characteristics. This distinctive particle morphology improves dimensional stability, flexural modulus and heat deflection thereby increasing the performance of many products including plastics, paints and coatings, construction materials, friction stability enhancement, ceramic and metallurgical applications.

In construction, Wollastonite is used as a substitute for asbestos in fire-resistant building products due to its low thermal conductivity and high aspect ratio structure. It improves flexural and impact strengths as an additive. In this field, Wollastonite finds application in interior and exterior construction boards, roof tiles, shaped insulation products, sheets, panels and sidings. For our experiment, we weigh 1 g of the powder and add it to 1X PBS (Phosphate buffer saline) solution and sediment it for 5 min to cut off the upper size limit since our microchannel is limited to 28 μm in height. After sedimentation, we withdraw some amount of sample and use this for impedance cytometry experiments.

3.4 Electrical Impedance Cytometry

Electrical impedance spectroscopy is a technique used to derive the dielectric parameters of particles by measuring the AC electrical properties of particles in suspension. It is most commonly employed in the field of biotechnology in cell sorting and counting [14] [15], protein engineering [16] and biomarker detection. We extend the advancements made in electrical impedance cytometry for particle analyzers to a miniaturized, low cost and precise instrumentation.

In microfluidic impedance-based cytometry, two electrodes are integrated into the walls of a microchannel. AC voltage is applied between these pair of electrodes inducing a current flow through the system. As a particle flows through the microchannel filled with electrolyte by means of capillary action and passes through the electrodes, it displaces the conductive fluid and alters the impedance and we measure this change as a voltage or current pulse. This change corresponds to the particle passing by and the magnitude is proportional to the amount of displaced fluid. Figure 3.9 presents a simplified schematic of an impedance cytometer with gold electrodes micropatterned onto a glass wafer in contact with a microfluidic channel. The voltage/current drop shown is seen as particles pass through the electrodes. The resulting peak information is extracted and used to analyze properties of various particles.

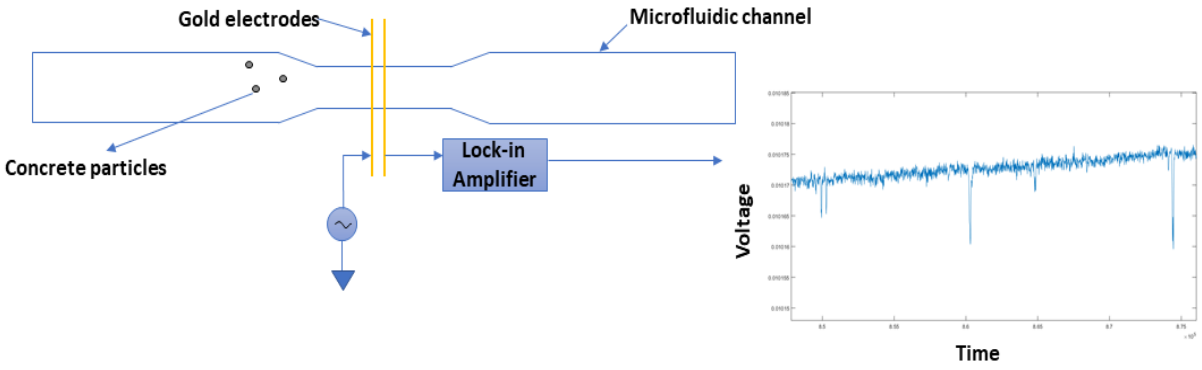

Figure 3.9. Simplified diagram of an impedance cytometer. Each peak corresponds to a single particle passing by.

The structure of the microfluidic cytometer in this paper is composed of a main channel and a sensing aperture. Electrical measurements were conducted across a wide range of frequencies to determine the suitable operating frequency. For our design, we assume an ideal polarizable electrode system with no faradic reactions since gold is used to fabricate the electrodes. When a voltage is applied across the two electrodes, it results in a double layer of ions with opposing polarity forming a boundary and acting as a capacitance, which is commonly referred to as the double-layer capacitance. A simplified circuit model proposed by Gawad et. al [17] to detect impedance change in the presence of particle along with the readout circuit is presented in Figure 3.10. The electrical equivalent circuit takes into consideration the channel resistance, i.e. the resistance of the electrolyte filled microchannel between the two electrodes (R_{sol}), two double layer capacitances (C_{dl}) which are formed at the interfaces of the electrolyte with the electrodes and are in series with the cell capacitance (C_{cell}) and membrane resistance (R_m).

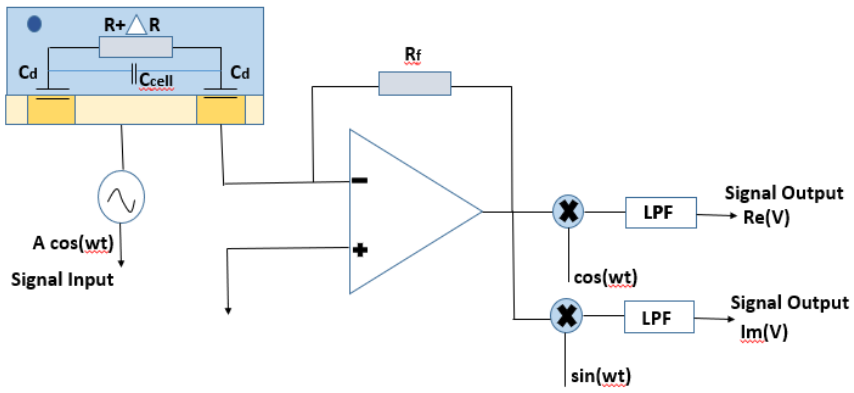

Fig 3.10 Equivalent circuit model of the electrode-electrolyte interface in the microchannel along with the readout circuit for measuring changes in resistance across the channel.

The change in impedance as each particle passes through is given by (Deblois and Bean 1970 [1]):

$$\Delta R = \frac{2\rho_{sol}\left(\tan^{-1}\left(\frac{d}{2\sqrt{\frac{Ac}{\pi}-\frac{d^2}{4}}}\right)\right)}{\pi\sqrt{\frac{Ac}{\pi}-\frac{d^2}{4}}} - \frac{d}{2Ac} \qquad (1)$$

Where *Ac* is the area of the channel and ρ_{sol} is the solution resistivity. Amplitude change of the signal from a particle passing through is given by:

$$\Delta I \approx \frac{\Delta R}{R^2}\, V_{in} \qquad (2)$$

3.5 Signal Processing

The signal measured at the output of the operational amplifier containing pulses corresponding to the passage of the particles is recorded. This data is carried on a sinusoidal modulation signal at a known excitation frequency and he voltage response was filtered to remove unwanted high frequency and low frequency noise. Using an algorithm to detrend and denoise the cytometry with minimal error, we detect the variation in the amplitude of the filtered signal.

The filtering and peak detection have been implemented using custom code written in MATLAB (Mathworks, USA). A major section of this algorithm was developed and analyzed by Xinnan Cao from our group [19]. After detrending and denoising the data, peak location was found out using the *findpeaks* [18] function in MATLAB®. Based on the peak locations we implemented a code to find real and imaginary value of each peak. These values were further used to calculate electrical parameters of each peak.

Chapter 4

Results and Discussion

We perform impedance cytometry measurements using 5ul of the sample prepared as explained in section 3.3. The sensor's response (v_s) for 500 kHz and 1 MHz operating frequencies was recorded at a sampling rate of 1.8kHz. The measured response was then analyzed with a program written in MATLAB and the voltage response of the channel is recovered using peak detection algorithm (section 3.5). Figure 4.1 shows the change in voltage for a single channel at 500 kHz ac for Wollastonite NYAD-400 particles where each pulse represents the passage of a particle through the channel.

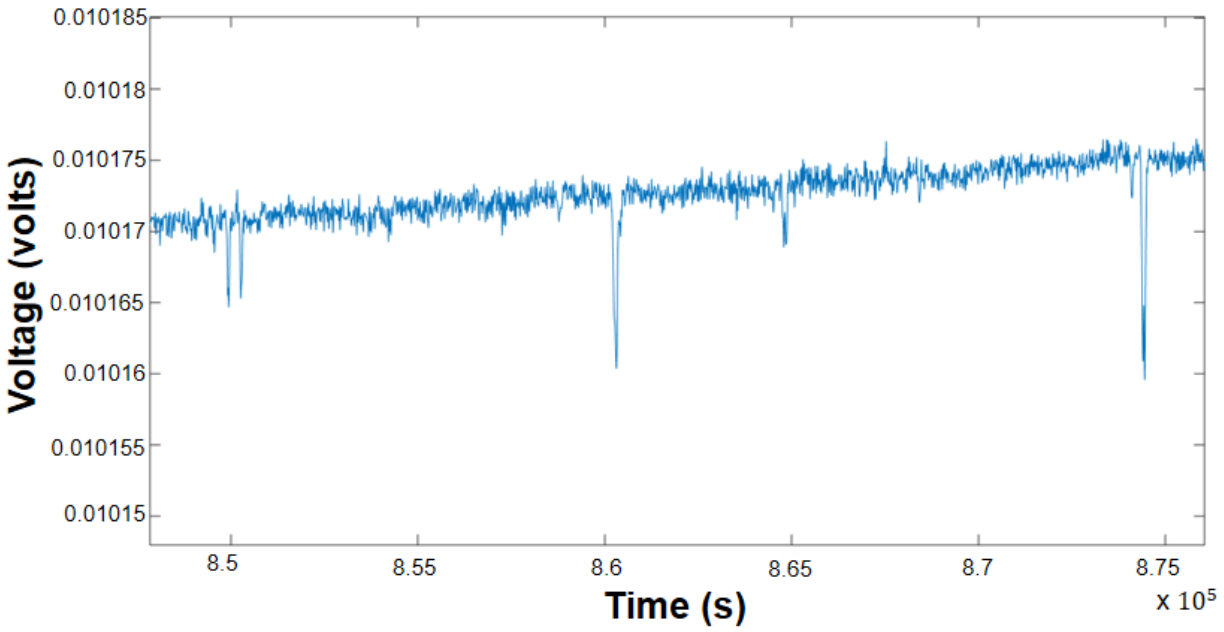

Figure 4.1 Each pulse represents passage of a particle across the electrodes

4.1 Detection of NYAD-400 particles

In order to determine the size of the particle that caused the change in impedance, it is important to understand the relationship between the change in voltage in response to the particle passing through the sensing channel. The change in impedance as each particle passes through the electrodes ΔR is calculated as,

$$I_{baseline} = \frac{V_{baseline}}{Gain} \quad (3)$$

$$\Delta V = \Delta R * I_{baseline} \quad (4)$$

$$\Delta R = \frac{\Delta V}{I_{baseline}} \quad (5)$$

where $I_{baseline}$ is the baseline current, $V_{baseline}$ is the baseline voltage and ΔV is the change in voltage as the particle passes through the channel.

To determine the size of the particle, we use the relation given by (Deblois and Bean 1970 [1]) between impedance change and diameter of the particle *d*,

$$\Delta R = \frac{2\rho_{sol}\left(\tan^{-1}\left(\frac{d}{2\sqrt{\frac{Ac}{\pi}-\frac{d^2}{4}}}\right)\right)}{\pi\sqrt{\frac{Ac}{\pi}-\frac{d^2}{4}}} - \frac{d}{2Ac}$$

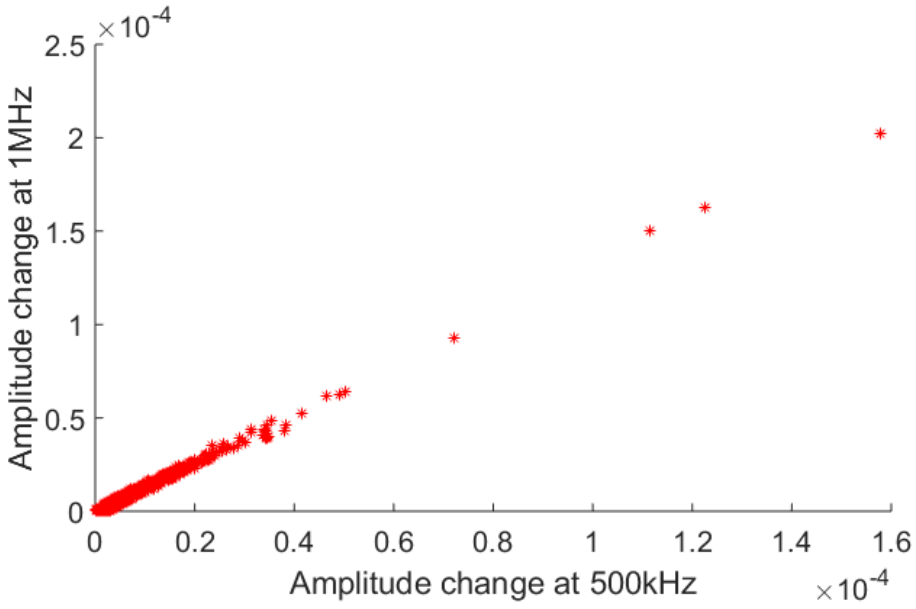

Figure 4.2 Scatter plot for amplitude change of Wollastonite NYAD-400 particles at 2 frequencies

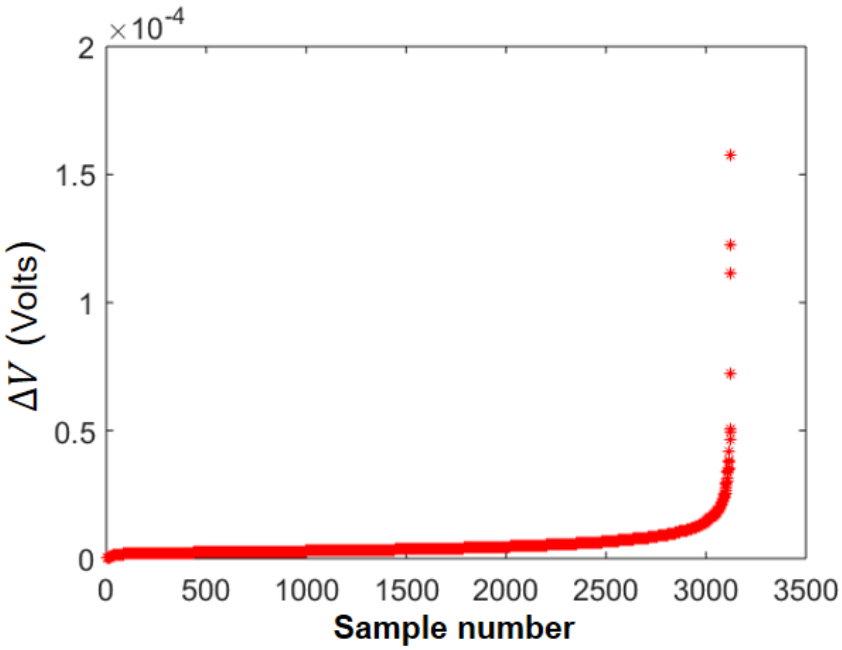

Figure 4.3 Plot shows number of particles in the sample and their corresponding ΔV at 500 kHz

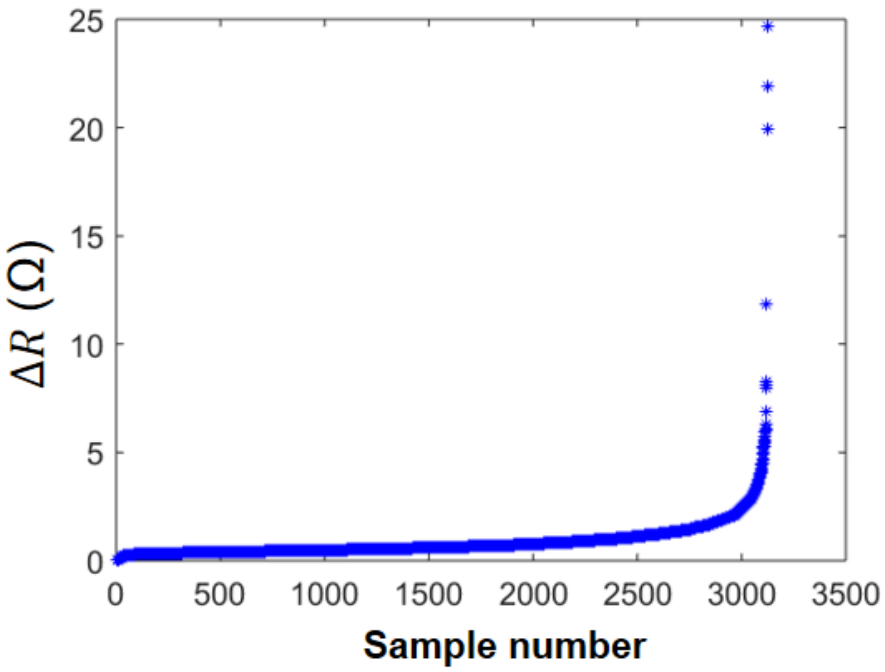

Figure 4.4 Plot shows number of particles in the sample
and their corresponding ΔR at 500 kHz

We run the measurement a total of five times in order to note the variation in measurement distribution. All of these measurements are run on one device to avoid device-to-device variations. For each of these runs, the sample is made each time by re-suspending the dry sample in 1X PBS allowing it to sediment for 5 min and then drawing 5ul of this dispersion to use in our impedance cytometry experiments.

Figures 4.2, 4.3 and 4.4 illustrates the results obtained for the first measurement which recorded a total of 3102 particles passing through the sensor device.

Figures 4.5 and 4.6 illustrates the results obtained for the second measurement which recorded a total of 2853 particles passing through the sensor device.

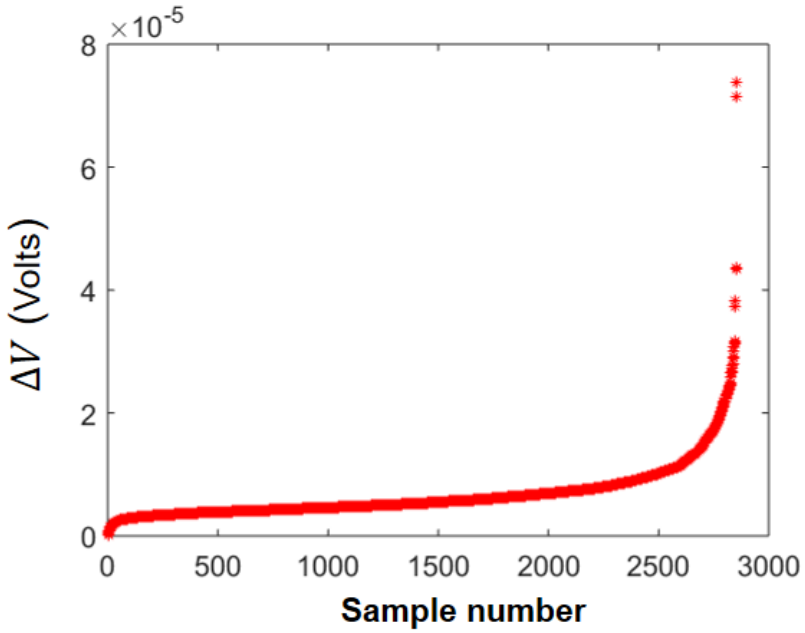

Figure 4.5 Plot shows number of particles in the sample and their corresponding ΔV at 500 kHz

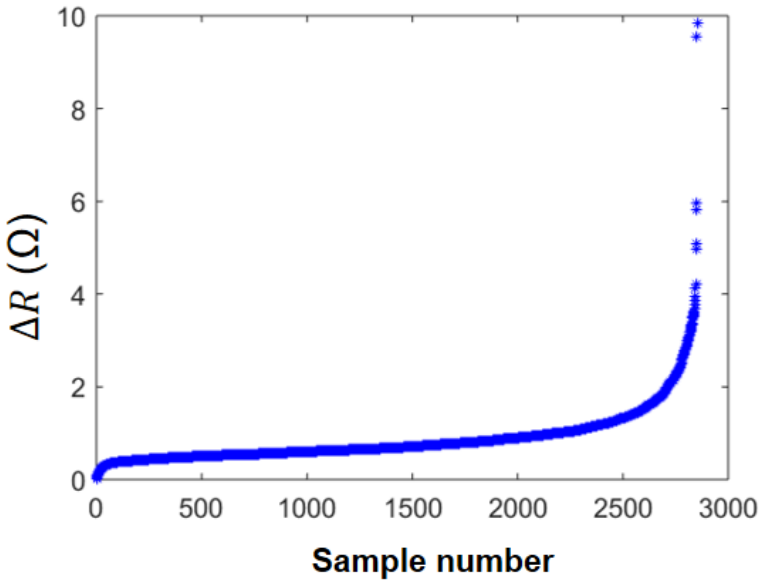

Figure 4.6 Plot shows number of particles in the sample and their corresponding ΔR at 500 kHz

Figures 4.7 and 4.8 illustrates the results obtained for the third measurement which recorded a total of 3119 particles passing through the sensor device.

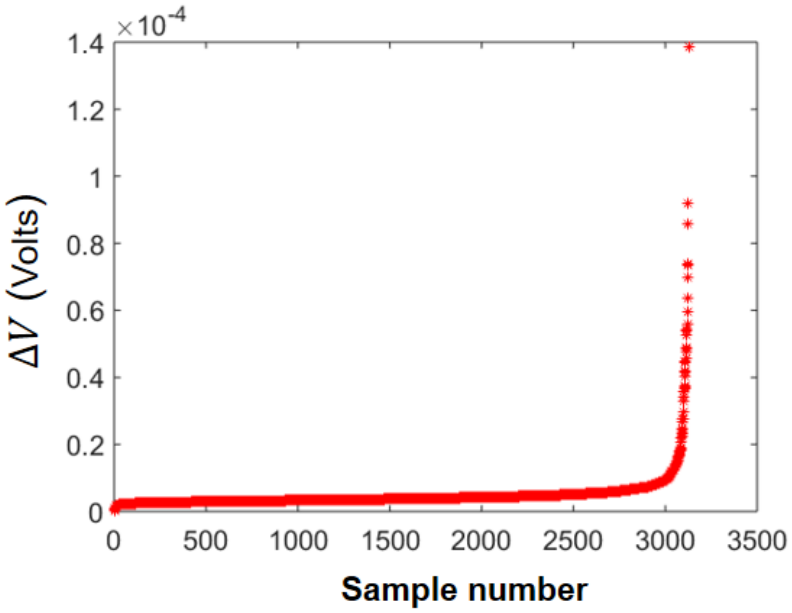

Figure 4.7 Plot shows number of particles in the sample and their corresponding ΔV at 500 kHz

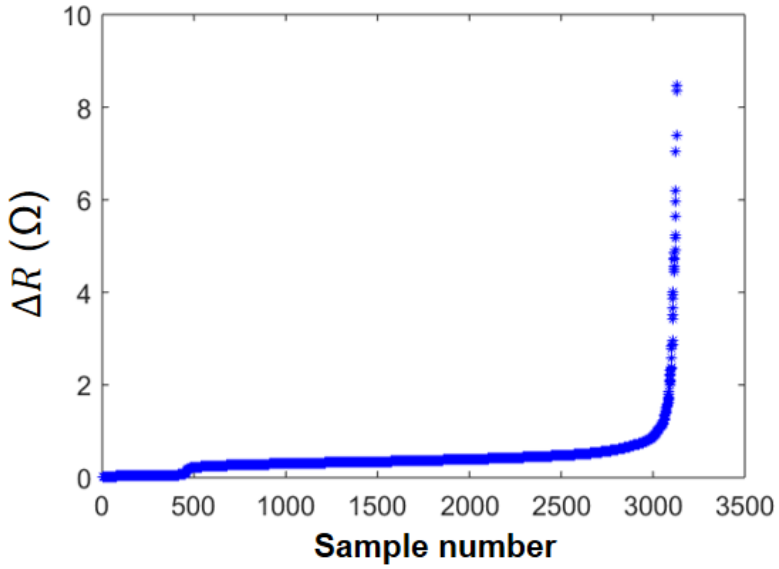

Figure 4.8 Plot shows number of particles in the sample and their corresponding ΔR at 500 kHz

Figures 4.9 and 4.10 illustrates the results obtained for the fourth measurement which recorded a total of 4286 particles passing through the sensor device.

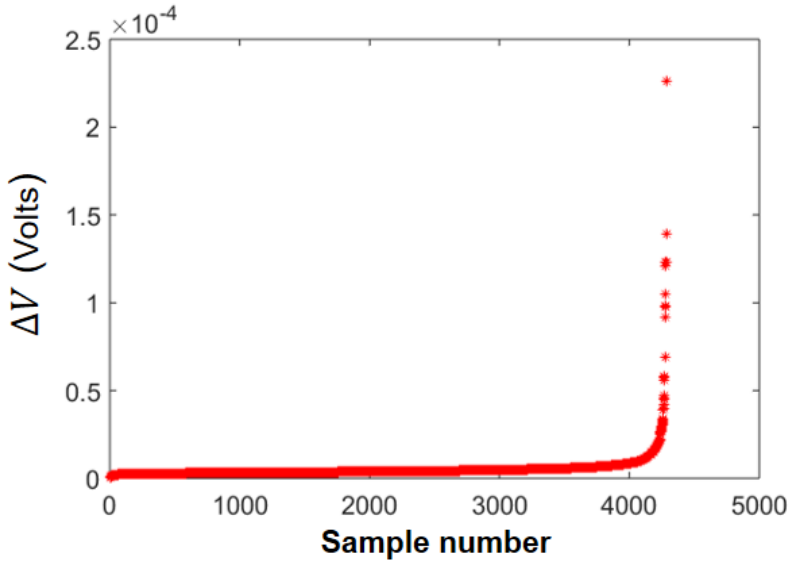

Figure 4.9 Plot shows number of particles in the sample and their corresponding ΔV at 500 kHz

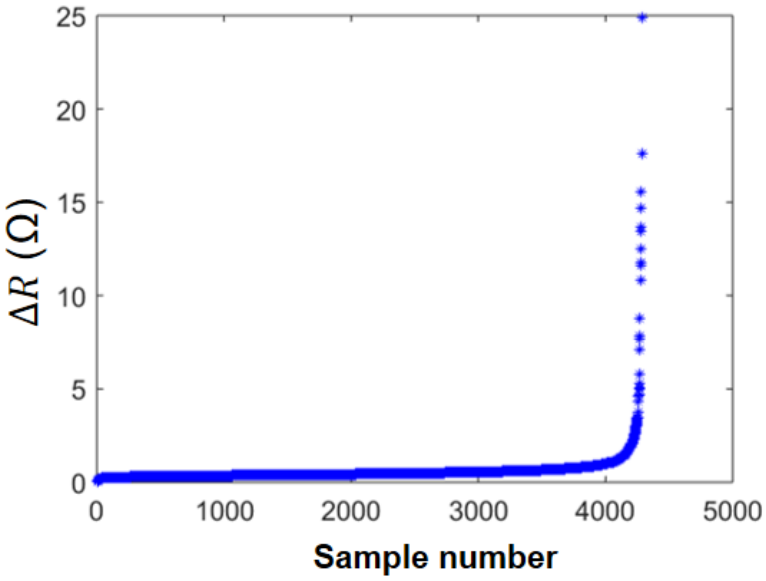

Figure 4.10 Plot shows number of particles in the sample and their corresponding ΔR at 500 kHz

Figures 4.11 and 4.12 illustrates the results obtained for the fifth measurement which recorded a total of 2633 particles passing through the sensor device.

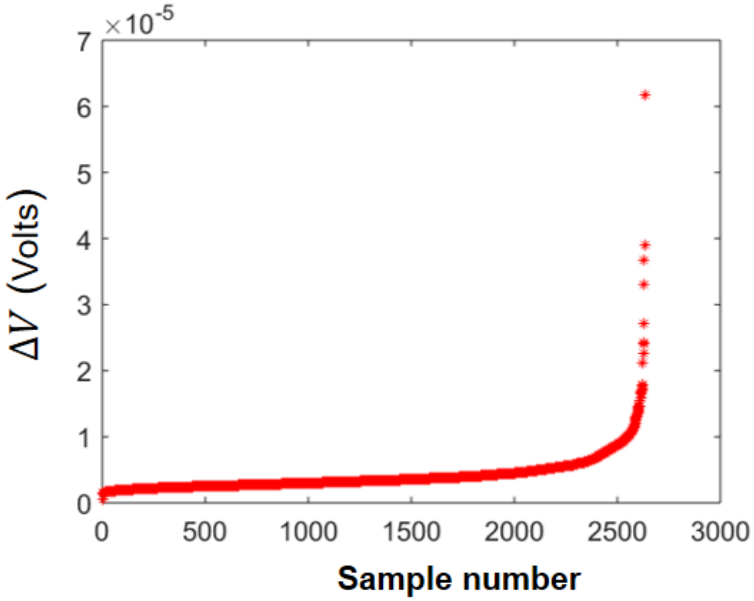

Figure 4.11 Plot shows number of particles in the sample and their corresponding ΔV at 500 kHz

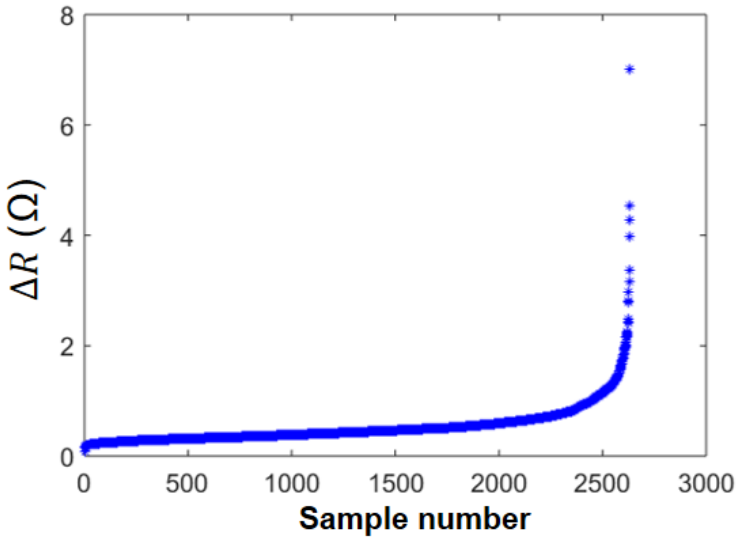

Figure 4.12 Plot shows number of particles in the sample and their corresponding ΔR at 500 kHz

4.1 Measurement analysis

A histogram is an accurate representation which aids in the visualization of the distribution of numerical data over a time period or a continuous interval. Figure 4.13 shows a histogram for 5 measurements to visualize the variation of each particle size and count in each measurement.

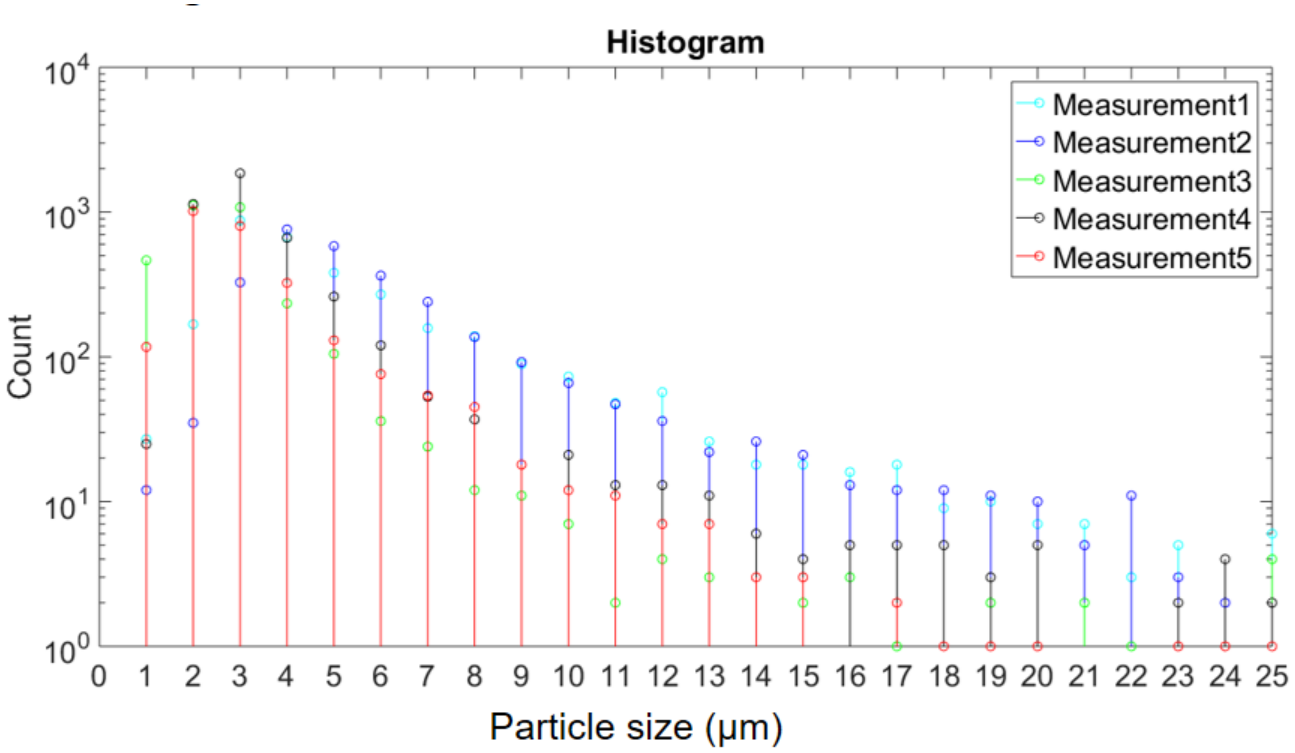

Figure 4.13 Histogram depicting variation in 5 measurements for each particle size and count

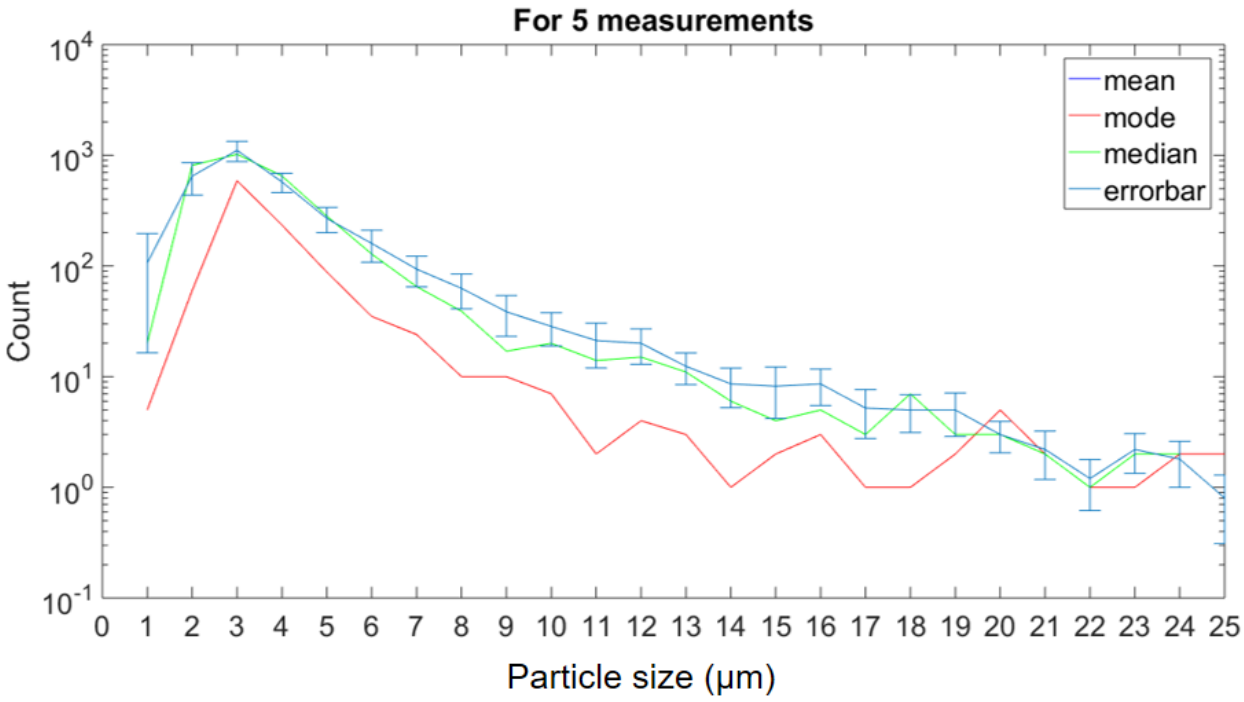

Figure 4.14 Variation in mean, mode, median with errors bars (standard error) for 5 measurements

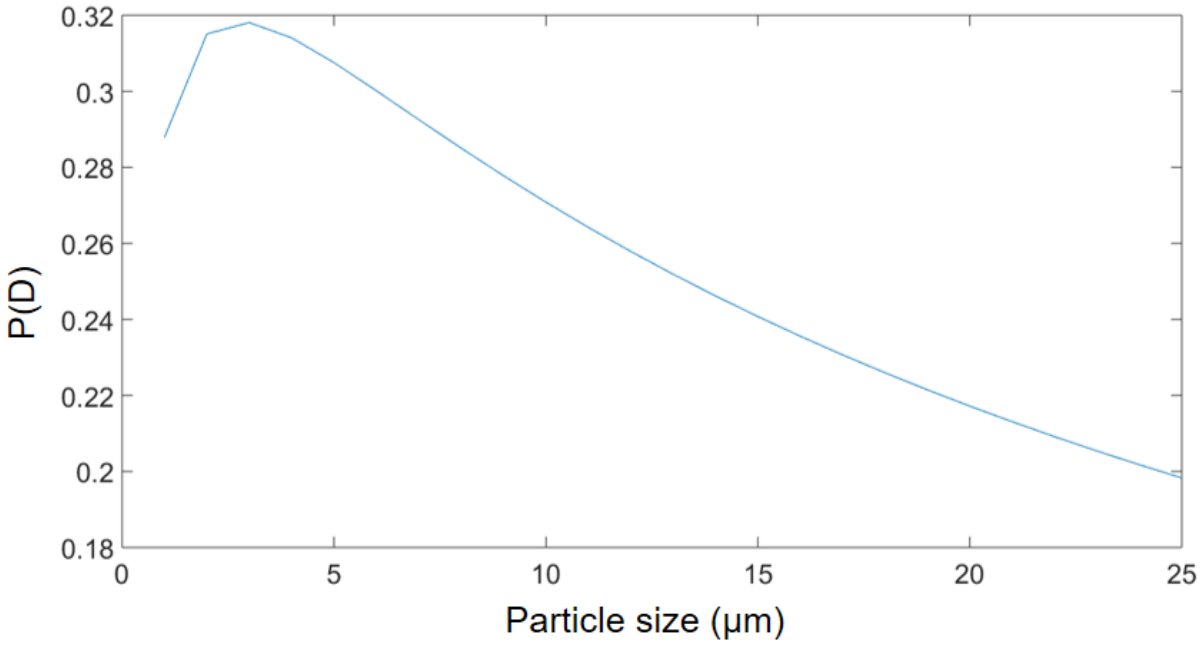

Figure 4.15 Lognormal distribution plot

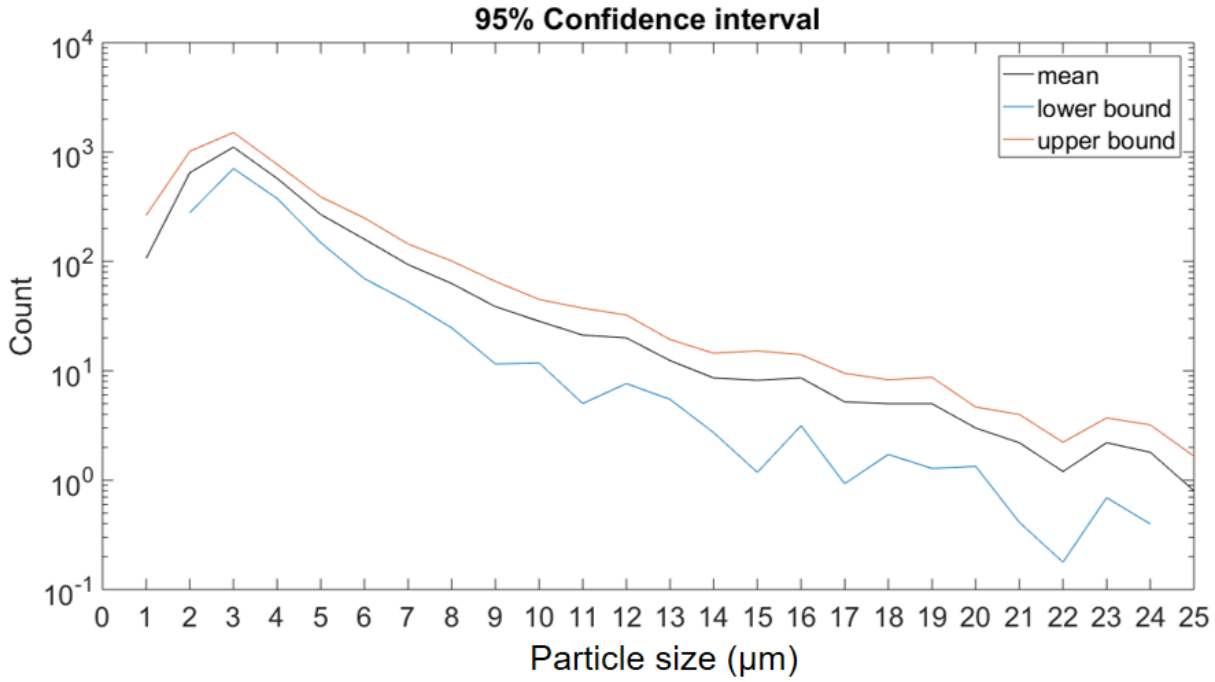

Figure 4.16 Confidence interval of 95% depicting the mean count for each particle size lies between the lower and upper bound shown in figure.

Chapter 5

Conclusion and Future Scope

A microscale ac Coulter counter for accurately measuring the count and size of standard Wollastonite NYAD 400 particles was designed and fabricated. The experimental results show a detection range greater than 1 μm and a count of up to 4k particles in a single run. Our device operates at low frequency which is desirable as such devices would require simple measurement instruments and signal processing. We were also able to effectively analyze impedance cytometry data and use electrical properties like amplitude change to characterize the particulate sample. This approach has minimal sample requirement of 1 g and low fabrication costs as compared to optical techniques for particle size characterization.

With optimization of this device, we envision detection ranges of <100 nm to 100s of microns with a count of over 10k particles in a single trial and a redesign of the electrode system to improve sensitivity and dynamic range. Future work will also focus on applying this tool to detecting a broad range of particulate samples thus eliminating bulky instrumentation and high production costs.

Chapter 6

Appendix

6.1 Oxygen Plasma Etching

Oxygen plasma refers to any plasma treatment that is performed by introducing oxygen to the plasma chamber. Oxygen(O_2) is the most common gas used in plasma cleaning technology due to its low cost and wide availability. It is introduced by utilizing an oxygen source on a plasma system. Oxygen gas is often used to clean surfaces prior to bonding. It may also be combined with other gases to etch a variety of materials such as plastic and rubber.

Oxygen gas is also used to clean non-metal materials such as glass, plastics and teflon. Like some other forms of plasma, oxygen can also clean organic materials and is capable of surface modification.

PDMS is generally hydrophobic in nature. Surface treatment exposes the (OH) groups at the surface of the PDMS substrate that when brought together form Si---O----Si covalent bonds. Thus oxygen plasma alters the surface properties of PDMS rendering it hydrophilic[24].

Bibliography

[1] DeBlois R W and Bean C P (1970), Counting and sizing of submicron particles by the resistive pulse technique, *Rev. Sci. Instrum*. **41** 909–916.

[2] Henriquez R R, Ito T, Sun L and Crooks R M (2004),The resurgence of Coulter counting for analyzing nanoscale objects, *Analyst* **129** 478–82.

[3] S. Zheng, M. Liu, and Y. C. Tai, "Micro coulter counters with platinum black electroplated electrodes for human blood cell sensing," Biomed. Microdevices, vol. 10, no. 2, pp. 221–231, 2008.

[4] Heng J B, Ho C, Kim T, Timp R, Aksimentiev A, Grinkova Y V, Sligar S, Schulten K and Timp G (2004), Sizing DNA using a nanometer-diameter pore, Biophys. J. **87** 2905–11.

[5] J. S. Lorenz, O. Oliver, C. Catalin, G. Joanne, and F. K. Ulrich, "Detecting DNA folding with nanocapillaries," Nano Lett., vol. 10, no. 7, pp. 2493–2497, 2010.

[6] Y. Wu, D. B. James, and A. Mahmoud, "Micromachined Coulter counter for dynamic impedance study of time sensitive cells," *Biomed. Microdevice*, vol. 14, no. 4, pp. 739–750, 2012.

[7] DeBlois R W and Wesley R K (1977) Sizes and concentrations of several type C oncornaviruses and bacteriophage T2 by the resistive-pulse technique J. Virol**. 23** 227–33.

[8] J. I. Zwicker, “Impedance-based flow cytometry for the measurement of microparticles”, Semin. Thromb. Hemost., vol. 36, no. 8, pp. 819–823, 2010.

[9] Zhang Z, Zhe J, Chandra S and Hu J (2005), An electronic pollen detection method using Coulter counting principle, *Atmos. Environ*. **39** 5446–53.

[10] Jagtiani A V, Zhe J, Hu J and Carletta J (2006), Detection and counting of micro-scale particles and pollen using a multi-aperture Coulter counter, *Meas. Sci. Technol.* **17** 1706.

[11] H. Bayley and C. R. Martin, “Resistive-pulse sensing-from microbes to molecules”, *Chem. Rev*., vol. 100, no. 7, pp. 2575–2594, 2000.

[12] Coulter W H 1953 Means for counting particles suspended in a fluid *US Patent* 2656508.

[13] Zheng S, Liu M and Tai Y C (2008), Micro coulter counters with platinum black electroplated electrodes for human blood cell sensing, *Biomed. Microdevices* **10** 221–31.

[14] MEMS-based Coulter counter for cell counting and sizing using multiple electrodes, Y Wu, J D Benson, J K Critser and M Almasri.

[15] Zhe J, Jagtiani A, Dutta P, Hu J and Carletta J 2006 A micromachined high throughput Coulter counter for bioparticle detection and counting *J.Micromech. Microeng.* **17** 304-13.

[16] “*Label-free protein detection using a microfluidic Coulter-counter device*”, Romen Rodriguez-Trujilloa, Mohammad A. Ajinea, Alice Orzana, Mikkel D. Mar b, Flemming Larsena, Casper H.Clausena, Winnie E. Svendsena.

[17] S. Gawad, L. Schild and Ph. Renaud, Micromachined impedance spectroscopy flow cytometer for cell analysis and particle sizing, *Lab on a Chip*, 2001, **1**,76-82.

[18] Find peaks function, *MATLAB*, Retrieved March 10, 2018.

[19] Cao X., Detrending and denoising of impedance cytometry data, Retrieved Rutgers University online libraries.

[20] An impedimetric approach for accurate particle sizing using a microfluidic Coulter counter, Ashish V Jagtiani, Joan Carletta and Jiang Zhe.

[21] M. Javanmard, R. W. Davis, A microfluidic platform for electrical detection of DNA hybridization, Sens.Actuators B: Chem 154(1) (2011) 22-27.

[22] Continuous scanning of the mobility and size distribution of charged clusters and nanometer particles in atmospheric air and the Balanced Scanning Mobility Analyzer BSMA H. Tammet

[23] Z. Lin, X. Cao, P. Xie, M. Liu and Mehdi Javanmard, PicoMolar level detection of protein biomarkers based on electronic sizing of bead aggregates: theoretical and experimental considerations. *Biomed Microdevices*. vol. 17, no. 6, pp. 119, 2015.

[24] S. H. Tan, N. Nguyen, and C. Chua, "Oxygen plasma treatment for reducing hydrophobicity of a sealed polydimethylsiloxane microchannel," pp. 1–9, 2010.

[25] Synthesis, characterization, and dispersion properties of hydroxyapatite prepared by mechanochemical–hydrothermal methods, Chun-Wei Chen, Charles S. Oakes, Kullaiah Byrappa, Richard E. Riman, Kelly Brown, Kevor S. TenHuisen and Victor F. Janas.

[26] Particle shape characterization and classification using automated microscopy and shape descriptors in batch manufacture of particulate solids Yang Zhang, Jing J. Liu, Lei Zhang, Jorge Calderon De Anda, Xue Z. Wang.

[27] A Microfluidic Impedance Cytometer on Printed Circuit Board for Low Cost Diagnosis, Jinhong Guo, Honggang Li, Yu Chen, and Yuejun Kang.

[28] A basic guide to particle characterization, 2015 Malvern Instruments Limited©.

[29] Single-cell microfluidic impedance cytometry: a review, Tao Sun, Hywel Morgan, Springer-Verlag 2010.

[30] Methodology for Determination of the Maximum Packing Fraction for Particle-Filled Polymer Suspensions, Tian Hao & Richard. E. Riman.

[31] Saleh O A and Sohn LL 2001 Quantitative sensing of nanoscale colloids using a microchip Coulter counter *Rev. Sci. Instrum.* **72** 4449.

[32] Morgan H, Sun T, Holmes D, Gawad S and Green N G 2007, Single cell dielectric spectroscopy *J.Phys.D: Appl. Phys.* **40** 61-70.

[33] Ayliffe H, Frazier A and Rabbitt R 1999 Electric impedance spectroscopy using microchannels with integrated metal electrodes *J. Microelectromech. Syst.* **8** 50-7.

[34] Satake D, Ebi H, Oku N, Matsuda K, Takao H, Ashiki M and Ishida M 2002 A sensor for blood cell counter using MEMS technology *Sensors Actuators B* **83** 77-81.

[35] Hoffman R and Britt W 1979 Flow-system measurement of cell impedance properties *J. Histochem. Cytochem.* **27** 234-40.

[36] Timmer B, Aparreboom W, Othuis W, Bergveld P and Berg A 2002 Optimization of an electrolyte conductivity detector for measuring low ion concentrations *Lab Chip* **2** 121-4.

[37] "Cytocoded passwords: BioMEMS based barcoding of biological samples for user authentication in microfluidic diagnostic devices" Gabriel Salles-Loustau, Tuan Le, Laleh Najafizadeh, Saman Zonouz, Mehdi Javanmard

[38] Electronic Quantification of Protein Biomarkers based on Bead Aggregate Sizing, Zhongtian Lin, Pengfei Xie, Xinnan Cao and Mehdi Javanmard.

[39] S. Emaminjed, M. Javanmard, R.W. Duton, R.W. Davis, Microfluidic diagnostic tool for the developing world: contactless impedance flow cytometry, *Lab on a Chip*, **12**(no. 21) (2012) 4499.

[40] Xie P., Cao X., Lin Z. and Javanmard M., Top-down fabrication meets bottom-up synthesis for nanoelectronic barcoding of microparticles. *Lab on a Chip*, 2017,**17**, 1939-1947.

[41] Elzone II 5390 Particle Size Analyzer Brochure_3, Micromeritics

[42] Wollastonite NYAD-400 Technical Data Sheet|IN-071-05-2|NYCO Minera.